Available online at www.sciencedirect.com
ScienceDirect
International Journal of Pharmaceutics 345 (2007) 95–100
INTERNATIONAL JOURNAL OF PHARMACEUTICS
www.elsevier.com/locate/ijpharm

# Phase characterization of indomethacin in binary solid dispersions with PVP VA64 or Myrj 52

Xin Wang [a], Hector Novoa de Armas [a], Norbert Blaton [b], Armand Michoel [b], Guy Van den Mooter [a,*]

[a] *Laboratorium voor Farmacotechnologie en Biofarmacie, Faculteit Farmaceutische Wetenschappen, Katholieke Universiteit Leuven, Campus Gasthuisberg O&N2 bus 921, B-3000 Leuven, Belgium*
[b] *Laboratorium voor Biokristallografie, Faculteit Farmaceutische Wetenschappen, Katholieke Universiteit Leuven, Campus Gasthuisberg O&N2 bus 822, B-3000 Leuven, Belgium*

Received 17 February 2007; received in revised form 17 May 2007; accepted 23 May 2007
Available online 29 May 2007

**Abstract**

In the present study the properties of binary solid dispersions made up of PVP VA64, Myrj 52 and indomethacin (IMC) are studied and characterized. The solid dispersions were prepared by dissolving the materials in dichloromethane, followed by solvent evaporation under reduced pressure at 55 °C in a rotavapor. Binary solid dispersions were characterized by standard and modulated temperature differential scanning calorimetry (MTDSC), thermogravimetry (TGA) and X-ray powder diffraction (XRPD). XRPD analysis showed that the initial IMC was in its γ-form, and that it was transformed to the β-form (reported to be a solvate) together with an amorphous fraction in the solid dispersions. A mixture of the β-form and amorphous IMC was also obtained in the binary systems containing less than 30% polymer. IMC without adding polymer was subjected to the same experimental procedures as in the solid dispersions, and used as a model to characterize the solid-state transformations. The following order of transitions was observed: from the initial γ-form, the β-form was obtained together with an amorphous component, then the crystalline β-form transforms into the α-form which melts and recrystallizes into the most stable γ-form.


*Keywords:* PVP VA64; Myrj 52; Indomethacin; Polymorphism; MTDSC; X-ray powder diffraction; Solid dispersions

## 1. Introduction

Compounds with poor aqueous solubility are increasingly posing challenges in the development of new drugs, because many new drug candidates discovered by combinatorial chemistry and high-throughput screening are poorly water-soluble (Ohara et al., 2005). Several pharmaceutical strategies are available to improve drug solubility, such as salt formation, micronization, and addition of solvents or surface-active agents. Formulation of solid dispersions is another strategy that can increase the solubility and dissolution rate of drugs (Chiou and Riegelman, 1971). Although the use of solid dispersions has been reported frequently in the pharmaceutical literature, only a few solid dispersion systems are used commercially. The main reason for this discrepancy is the possible physical instability of these structures that can be metastable (Serajuddin, 1999; Leuner and Dressman, 2000). Phase separation, crystal growth or conversion from the amorphous (metastable) to the crystalline state during storage, inevitably results in decreased solubility and dissolution rate. However, the presence of a carrier (polymer) is often adequate to prevent recrystallization (Motsumoto and Zografi, 1999; Van den Mooter et al., 2001).

The interest in using surface-active agents for poorly water-soluble drugs increased in recent years (Serajuddin, 1999). Gelucire 44/14, Vitamin E TPGS NF and polysorbate 80 are examples of such carriers. Furthermore, it has been reported that a solid dispersion made up of polyethylene glycol and polysorbate 80 could improve the dissolution rate and enhance the bioavailability of LAB687, a poorly water-soluble drug (Dannenfelser et al., 2004). The bioavailability of this kind of solid dispersion showed a 10-fold increase compared to the dry blend of micronized drug with microcrystalline cellulose. In addition the solid dispersion system was physically and

* Corresponding author. Tel.: +32 16 330304; fax: +32 16 330305.
*E-mail address:* guy.vandenmooter@pharm.kuleuven.be (G. Van den Mooter).

0378-5173/$ – see front matter © 2007 Elsevier B.V. All rights reserved.
doi:10.1016/j.ijpharm.2007.05.046

chemically stable for at least 16 months at 25 °C/60% RH.

Indomethacin (IMC) is a widely used non-steroidal anti-inflammatory drug. Because of its low water solubility (5 μg/ml, Hancock and Parks, 2000), IMC is often used as a model drug in the study of solid dispersions. It was reported that IMC shows a complicated polymorphic behavior (Lin, 1992; Slavin et al., 2002). The regularly obtained true polymorphs are γ-form (also called form I, mp: 160–161.5 °C) (Sungthongjeen et al., 2004) and α-form (also called form II, mp: 150–155 °C) (Slavin et al., 2002; Otsuka et al., 2003). The remaining true polymorphs (called forms IV, VI and VII) are metastable and readily transform to α-form or γ-form. Slavin et al. (2002) reported that the IMC β-form (also called form V) is a solvated form which can be formed readily from a wide range of solvents, such as cyclohexanone, $C_6H_6$, $CHCl_3$, $CH_2Cl_2$, $CCl_4$ and THF, under high supersaturation conditions. The amorphous form, the γ-form and the α-form of IMC have been examined extensively by many other authors (Taylor and Zografi, 1997; Yoshioka et al., 1994; Otsuka et al., 2000, 2003; Takeuchi et al., 2005; Fujii et al., 2005). During storage, amorphous IMC can form one of the two polymorphic forms: the more thermodynamically stable γ-form crystallizes well below $T_g$ and the less stable α-form crystallizes above $T_g$ (Yoshioka et al., 1994).

The aim of the present study is to investigate the phase behavior of IMC in binary solid dispersions with PVP VA64 (polymer) or Myrj 52 (surface-active agent).

## 2. Materials and methods

### 2.1. Materials

PVP VA64 was obtained from BASF (Germany) and Myrj 52 was obtained from Uniqema (Belgium). IMC was purchased from AlphaPharma (Belgium). Dichloromethane (Acros, Belgium) was of HPLC grade.

### 2.2. Preparation of solid dispersions by co-evaporation

Binary solid dispersions were prepared by dissolving different amounts of IMC powder, and PVP VA64 (PVP VA64–IMC) or Myrj 52 (Myrj 52–IMC) in dichloromethane. This was followed by evaporation under reduced pressure of the solvent at 55 °C in a rotavapor (Buchi, Switzerland). The solid dispersions were subsequently stored in vacuum over $P_2O_5$, and dried until constant weight. Afterwards, they were ground in a mortar, sieved (range 235–350 μm) and analyzed. XRPD showed no difference in the samples due to the grinding process.

### 2.3. Hot-stage microscopy

Hot-stage microscopy was performed using an Olympus BX51 (Olympus Optical Co. Ltd., Tokyo, Japan) polarizing optical microscope equipped with a LINKMAN THMS600 hot stage (Linkman Scientific Instruments Ltd., Surrey, England) and LINKMAN TMS94 programmable temperature controller. Samples were heated at 2 °C/min from room temperature to 190 °C.

### 2.4. DSC and MTDSC

MTDSC measurements were carried out using a 2920 Modulated DSC (TA Instruments, UK), equipped with a refrigerated cooling system (RCS). The samples were analyzed using aluminum open pans and each sample was scanned twice from 25 °C to 200 °C. The amplitude used was 0.212 K, the period 40 s and the underlying heating rate 2 °C/min. Octadecane, benzoic acid and indium standards were used to calibrate the DSC temperature scale; the enthalpic response was calibrated with indium. Heat capacity was calibrated with sapphire. Validation of temperature, enthalpy and heat capacity measurement was performed using the same standard materials. DSC curves were analyzed using the software Universal Analysis 2000 v.4.1D (TA Instruments, UK).

### 2.5. TGA

Thermogravimetric analysis was performed with a TGA Q500 (TA Instruments, Leatherhead, UK) using a dry nitrogen purge of 100 ml/min. A 8 mg of 100% treated IMC sample was placed in a 100 μl platinum cup and measured from 20 °C to 200 °C with a heating rate of 5 °C/min.

### 2.6. X-ray powder diffraction (XRPD)

XRPD was performed with a computer controlled Philips PW1710 (Bragg–Brentano geometry) diffractometer (Philips, The Netherlands) with a Ni Filtered Cu Kα radiation (λ = 1.5418 Å) and a system of diverging, scattering and receiving slits of 1/4°, 0.2 mm and 1/4°, respectively. The diffraction pattern was recorded in the interval $3° < 2\theta < 40°$ in a step scan mode of 0.02° per step every second. The instrument generator (PW1130/00) was powered at a voltage of 40 kV and a current of 32 mA. The powder samples were ground in an agate mortar and side loaded in the sample holder. Throughout the experiment the ambient temperature was maintained at 25 ± 1 °C. The diffractograms were analyzed using the WinPLOTR program, version March/2005 (Roisnel and Rodriguez-Carvajal, 2001).

### 2.7. High temperature X-ray powder diffraction (HT-XRPD)

HT-XRPD patterns were recorded on a BRUKER D8VARIO/VANTEC (Bruker, Germany) X-ray powder diffractometer (Cu $K\alpha_1$ radiation: λ = 1.54059 Å; operated at 40 kV and 40 mA; exit slit 1.0 mm, 2.5° soller slit) fitted with a Johannson type curved Ge(1 1 1) focusing primary monochromator and a VANTEC position sensitive detector (12° window configured). The instrument was calibrated employing a quartz standard. An MRI capillary furnace was used as heating device. The powder of treated IMC was difficult to prepare in a capillary due to its sticky nature. For this reason a rather large capillary (1.0 mm inner diameter, Hilgenberg

glass no. 14) was used. Data were collected in transmission geometry over a $2\theta$ range of 2–40°, with a step size of 0.016° and as counting time 0.3 s/step. Each measurement took 11 min in total. In addition, a delay time of 30 s was introduced before starting a measurement. Measurements were made every 5 °C between 30 °C and 140 °C. From this temperature onwards a measurement was made every 2 °C up to 180 °C. The ramping rate was 1 °C/min in each case. The capillary was rotated during measurement. The measurements were carried out with the software DIFFRAC®plus BASIC. The diffractograms were analyzed using the WinPLOTR program, version March/2005 (Roisnel and Rodriguez-Carvajal, 2001).

## 3. Results and discussion

IMC exhibits different polymorphic and pseudopolymorphic forms (also called solvates), among them: α-form, β-form and γ-form. The β-form is reported to be a solvate obtained from different types of solvents (Lin, 1992; Otsuka et al., 2003). The starting IMC used in our experiments corresponds to the γ-form (reported diffraction lines in the entry PDF 40-1710 in the Powder Diffraction File database (ICDD, 2005)).

Fig. 1 shows the XRPD diffractograms of binary solid dispersions made of γ-form IMC and PVP VA64. Diffraction peaks are present only in the solid dispersions 90% IMC/10% PVP VA64 and 80% IMC/20% PVP VA64. When the PVP VA64 content is higher than 30%, no diffraction peaks in the diffractograms and no melting endotherms in the DSC curves (Fig. 2) can be found. This means that IMC is molecularly dispersed in the polymeric matrix, existing as an amorphous entity in the solid dispersions and does not recrystallize or form polymorphs during heating. It is important to notice that diffraction peaks in the dispersions containing 80% and 90% IMC correspond to the β-form.

In order to investigate the polymorphic transformations that occur during preparation of the solid dispersions and the influence of the polymers in the possible phase transformations, the initial IMC γ-form was treated as in the solid dispersions but without adding polymer (referred as "treated IMC"). Fig. 1 also shows, besides the PVP VA64–IMC binary solid dispersions, the XRPD diffractograms of pure the γ-IMC and the treated IMC. Comparing the diffractogram of treated IMC with the data for the IMC polymorphs in the Powder Diffraction File database (ICDD, 2005), it can be concluded that the starting IMC γ-form has been transformed into the β-form (entry PDF 39-1884). Also an amorphous fraction is present. The amorphous content in the treated IMC was estimated from XRPD data in two steps. First the instrumental background contribution to the whole XRPD pattern was spline-interpolated. Subsequently, the surface of the crystalline peaks of IMC β-form and the amorphous halo were differentiated for integration and subtracted from the whole XRPD pattern. The amorphous content found in the treated IMC was 60%.

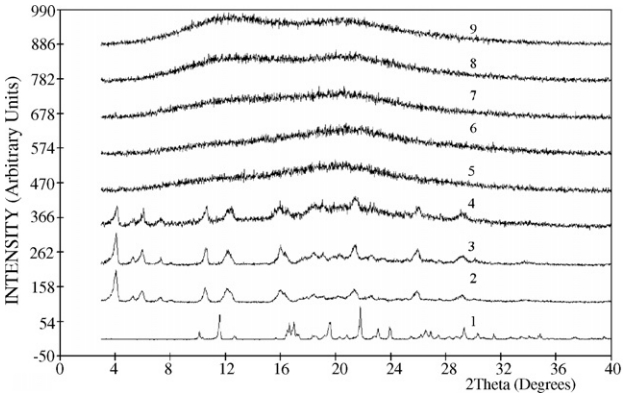


Fig. 1. X-ray powder diffraction curves of pure IMC (γ-form) (1), treated IMC (2) and PVP VA64–IMC solid dispersions with 90% IMC/10% PVP VA64 (3), 80% IMC/20% PVP VA64 (4), 70% IMC/30% PVP VA64 (5), 60% IMC/40% PVP VA64 (6), 40% IMC/60% PVP VA64 (7), 20% IMC/80% PVP VA64 (8), and 10% IMC/90% PVP VA64 (9).

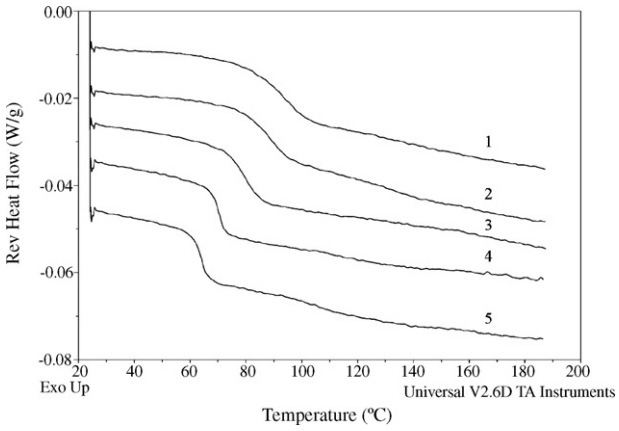


Fig. 2. Reversing heat flow curves of PVP VA64–IMC solid dispersions: 10% IMC/90% PVP VA64 (1), 20% IMC/80% PVP VA64 (2), 40% IMC/60% PVP VA64 (3), 60% IMC/40% PVP VA64 (4), and 70% IMC/30% PVP VA64 (5).

Fig. 3 shows the DSC curves of pure γ-IMC and treated IMC. Only one melting peak at 160 °C in the DSC curve of pure γ-IMC is observed. Endothermic and exothermic peaks are noticed in the interval 80–120 °C in the DSC curve of treated IMC. The first endotherm (ca. 86 °C) may be due to the loss of solvent of the β-form, as confirmed by TGA analysis (Fig. 4). The weight loss of 3.66% does not correspond to stoichiometrically bounded $CH_2Cl_2$. A possible explanation is that the solvent is adsorbed to the present amorphous fraction. The exothermic peak present

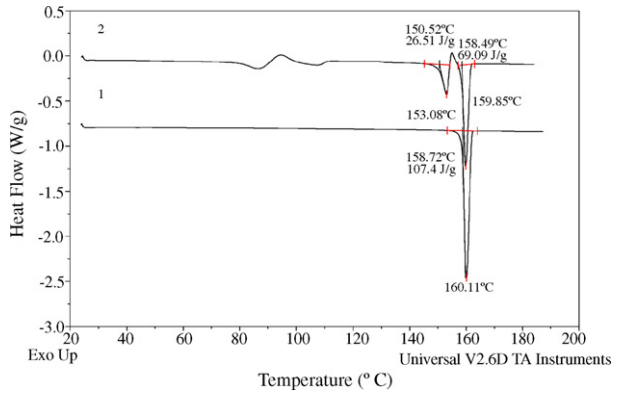


Fig. 3. DSC curves of pure IMC (γ-form) (1) and treated IMC (2).

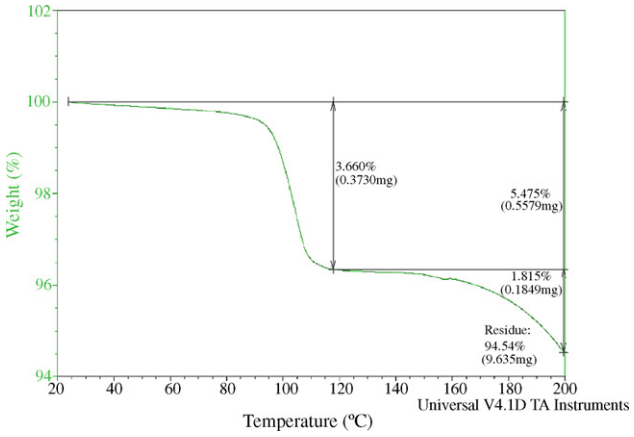


Fig. 4. TGA curve of treated IMC.

at ca. 92 °C could be explained as a partial recrystallization of the amorphous part.

On heating up to 120 °C, corresponding to the end of the loss of solvent process observed in the DSC/TGA experiments, the β-form fraction in the treated IMC transforms into the α-form. This was demonstrated by heating during 24 h a XRPD sample holder containing the treated IMC powder sample in a hot stage until a temperature just below 120 °C (Fig. 5A). Furthermore, when the treated IMC was heated to 120 °C, then cooled to RT and reheated again to 120 °C, the endo- and exothermic peaks between 80 °C and 120 °C disappeared. However, the lost solvent observed in the TGA analysis of the β-form is from an adsorbed nature rather than solvent incorporated into the crystal structure. In general, the loss of a solvent molecule in a solvate happens at higher temperatures because of the strong interactions (e.g. hydrogen bonds) between the solvent and the host molecule (Brittain, 1999). The adsorbed solvent, mostly present at the surface of the particles, is lost by evaporation at early temperatures. As observed in the TGA analysis, the loss of mass in the β-form starts as early as about 30 °C, not surprising due to the low boiling point of methylene chloride (39.8 °C), suggesting that this solvent is not really involved in any internal strong interaction. In Lin (1992) all the solvates, crystallized from different solvents having quiet different molecular structures (e.g. $C_6H_6$ and $CH_2Cl_2$), are all called the β-form. This could suggest that in the crystal structure of IMC β-form the internal voids would be always occupied by different size molecules, without forming any interaction (or very weak ones) with the IMC host molecule, the so called isomorphous solvates. But this is not the case, since the desolvated IMC β-form shows a different diffractogram (the different crystalline γ-form, Fig. 5A and B), while for an isomorphous solvate the same diffractogram would be expected after desolvation. This is in contradiction with the diffractograms shown in Lin (1992). Different solvated forms from different solvents should have different diffractograms (unless they are isomorphous desolvates). Based on our experimental indications and analysis of literature, we suggest that the solvates collectively named the IMC β-form are in fact a same distinct true polymorph and not a group of solvates. The knowledge of the IMC β-form crystal structure would firmly clarify the relationship with the host molecule and the different possible solvates, if they are really present. A search in the latest version of the crystal structure database CSD (version 5.28, Cambridge Crystallographic Data Centre, UK) gave no crystal structure reported for this crystalline form of IMC. Our attempts to obtain suitable crystals for single crystal diffraction of IMC β-form failed.

The amorphous fraction present together with the IMC α-form (Fig. 5A, diffractogram a), and calculated as done for β-form IMC, decreases to 50%. This explains the small exotherm at about 95 °C as a partial crystallization of the amorphous phase into the α-form. On the other hand, the DSC curve in Fig. 3 shows that after the IMC β-form transforms into α-form, it further recrystallizes into a new form that melts at 158.5 °C. This highest melting temperature indicates that the new form corresponds to a more stable form of IMC (suggested to be the γ-form by the value of the melting point). The TGA analysis shows that the final product starts to decompose at 170 °C.

In order to investigate these polymorphic transformations in one full cycle, and clearly identify the phases that exist at each

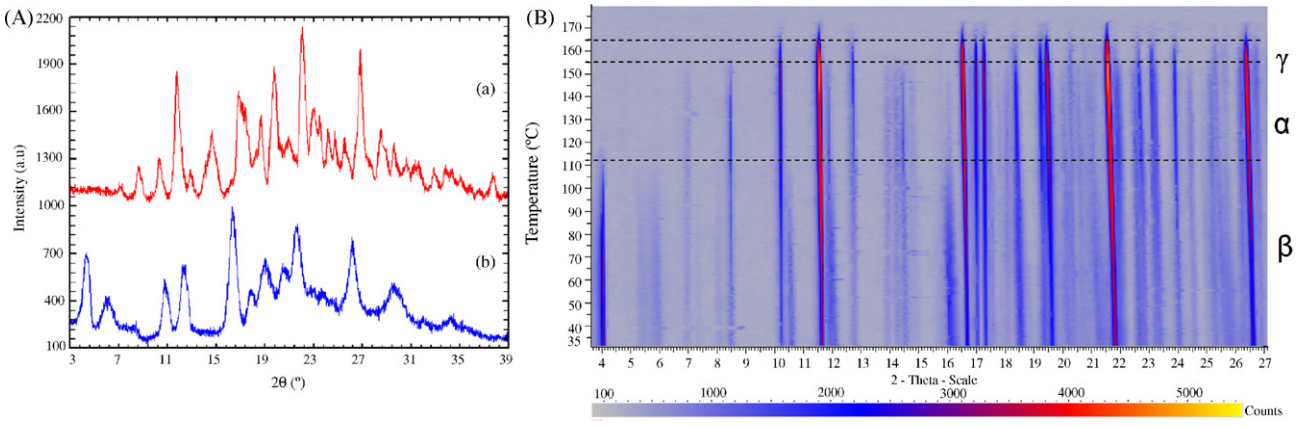


Fig. 5. High temperature X-ray powder diffraction experiments: (A) X-ray powder diffraction curves of the IMC β-form before heating (b) and after heating at 120 °C during 10 min (a, α-form). (B) Simulated Guinier film plots of the diffractograms between RT and 170 °C, showing the phase transitions starting by the treated IMC (β-form).

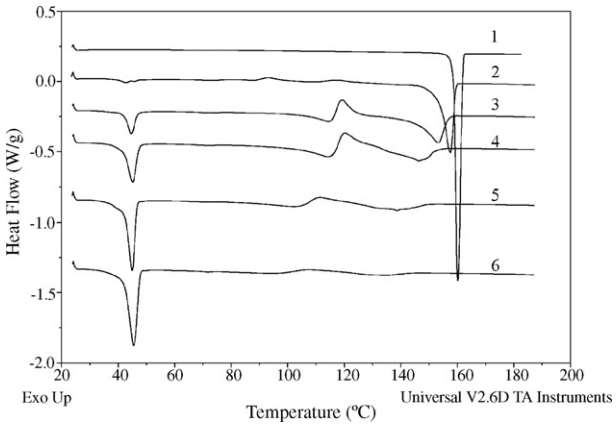


Fig. 6. Heat flow curves of solid dispersions of Myrj 52 and IMC: pure γ-IMC (1), 90% IMC/10% Myrj 52 (2), 80% IMC/20% Myrj 52 (3), 70% IMC/30% Myrj 52 (4), 60% IMC/40% Myrj 52 (5), and 50% IMC/50% Myrj 52 (6).

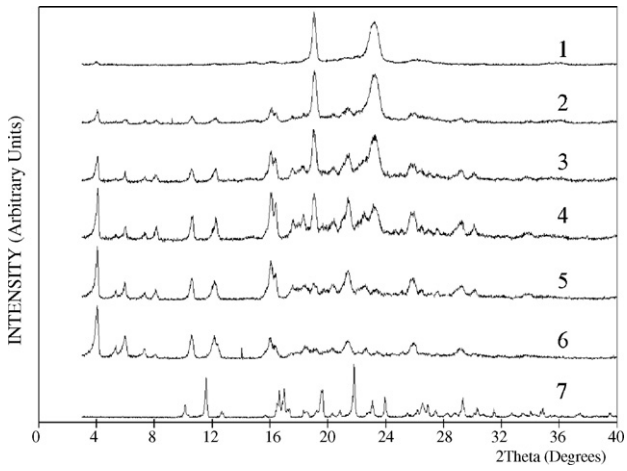


Fig. 7. X-ray powder diffraction curves of Myrj 52 and IMC solid dispersions: 10% IMC/90% Myrj 52 (1), 30% IMC/70% Myrj 52 (2), 50% IMC/50% Myrj 52 (3), 70% IMC/30% Myrj 52 (4), 90% IMC/10% Myrj 52 (5), treated IMC (6), and pure γ-IMC (7).

temperature, the treated IMC was subjected to HT-XRPD experiments. The iso-intensity plot in Fig. 5B confirms the phase transitions in the following order: the β-form transforms into the α-form and then recrystallizes into the γ-form. From Fig. 5B it can be seen that two characteristic diffraction peaks (as reported in the PDF-2 database) of the IMC β-form at $2\theta$ (°) = 3.95 and 5.80 fully disappear at 120 °C. When the γ-form is formed from the α-form above 155 °C, the peaks of the α-form at $2\theta$ (°) = 7.00 and 8.50 are no longer present. Only those corresponding to the γ-form ($2\theta$ (°) = 10.17 and 11.63) remain until decomposition of the sample at 170 °C.

Figs. 6 and 7 represent DSC and XRPD results of binary systems composed of Myrj 52 and IMC. All the diffractograms show the β-form and the amorphous IMC fraction in the solid dispersions at room temperature. Also the diffraction peaks of the Myrj 52 are present in all the diffractograms. In the DSC curves the endotherm corresponding to the melt of Myrj 52 is always present besides the endotherms from the different IMC polymorphs. This indicates that in the binary solid dispersions both compounds form at least two separate phases, one of Myrj 52 and one of IMC. DSC analysis showed a melting transition at about 45 °C corresponding to the melt of the polymer. The DSC curve from 90% IMC and 10% Myrj 52 of Fig. 6 resembles that of the treated IMC in Fig. 3. The recrystallization of the β-form into the α-form happens at lower temperature since the melting of the α-form occurs at lower temperatures. Also the recrystallization temperature of the polymorphic transition from the α-form to the γ-form, as well as the melt of the γ-form, shifts to lower temperatures.

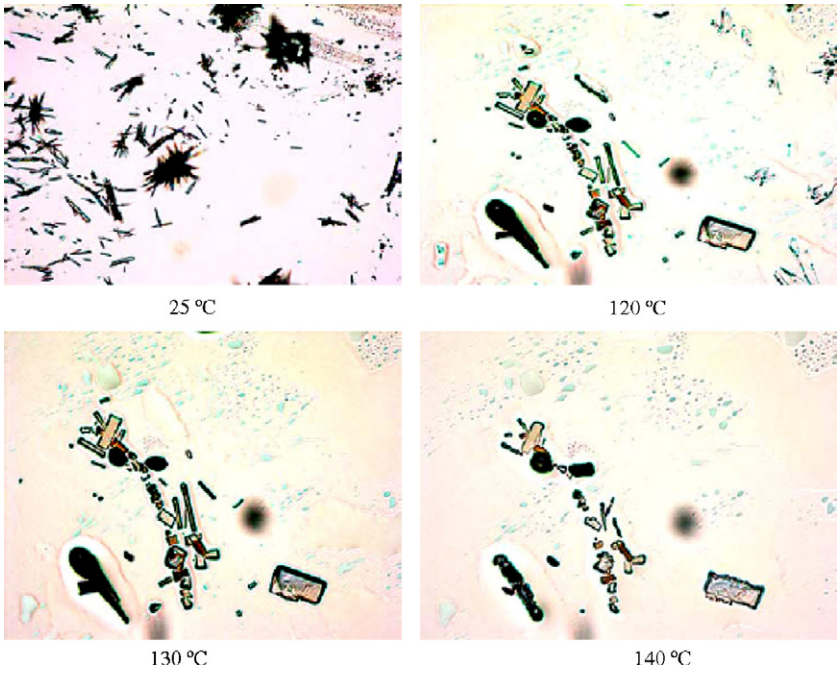


Fig. 8. HSM photos of 70% IMC/30% Myrj 52 dispersion.

Fig. 8 shows HSM photographs of 70% IMC/30% Mirj dispersion at RT and at temperatures above 120 °C. In Fig. 8 two different types of crystals were observed: needles and rhombic plates. Needles are the typical habit for α-form or β-form crystals and rhombic plates for the γ-form crystals (Slavin et al., 2002). It can be seen from the photographs, that rhombic plate crystals were recrystallized from the fine needles from 120 °C. The presence of Myrj 52 thermodynamically accelerates the recrystallization of IMC β-form into the γ-form. This behavior is clearly different from that in the absence of Myrj as depicted in Fig. 3.

## 4. Conclusion

IMC solid dispersions show a complex thermal behavior with polymorphic transformations. Although solid dispersions were prepared starting from the γ-form of IMC, it was transformed during solid dispersion formation to the β-form together with an amorphous fraction. The order of polymorphic transformations in the "treated IMC" was studied using DSC and HT-XRPD. It was observed that during heating IMC transformed from the β-form to the α-form and then recrystallized into the γ-form. In solid dispersions of PVP VA64–IMC having 30% or higher concentration of the polymer, the system is fully amorphous. Hence the drug is molecularly dispersed in the polymeric matrix. For these solid dispersions having a concentration of the drug lower than 70%, the IMC in its β-form is observed. In solid dispersions made of Myrj 52–IMC, the surfactant accelerates the recrystallization of IMC β-form into the γ-form.

## Acknowledgements

The authors would like to thank Bruker AXS GmbH for their help in the data collection of the high temperature transformations of IMC in their application labs in Karlsruhe (Germany). GVDM acknowledges financial support from the K.U. Leuven (OT 03/60).

## References

Brittain, H.G., 1999. Polymorphism in Pharmaceutical Solids. Marcel Dekker Inc., New York.

Chiou, W.L., Riegelman, S., 1971. Pharmaceutical applications of solid dispersion systems. J. Pharm. Sci. 60, 1281–1302.

Dannenfelser, R., He, H., Joshi, Y., Bateman, S., Serajuddin, A.T.M., 2004. Development of clinic dosage forms of a poorly water soluble drug. I. Application of polyethylene glycol–polysorbate 80 solid dispersion carrier system. J. Pharm. Sci. 93, 1165–1175.

Fujii, M., Okada, H., Shibata, Y., Teramachi, H., Kondoh, M., Watanabe, Y., 2005. Preparation, characterization, and tableting of a solid dispersion of indomethacin with crosspovidone. Int. J. Pharm. 293, 145–153.

Hancock, B.C., Parks, M., 2000. What is the true solubility advantage for amorphous pharmaceuticals? Pharm. Res. 74, 397–404.

Leuner, C., Dressman, J., 2000. Improving drug solubility for oral delivery using solid dispersions. Eur. J. Pharm. Biopharm. 50, 47–60.

Lin, S., 1992. Isolation and solid-state characteristics of a new crystal form of indomethacin. J. Pharm. Sci. 81, 572–576.

Motsumoto, T., Zografi, G., 1999. Physical properties of solid molecular dispersions of indomethacin with PVP and PVP VA in relation to indomethacin crystallization. Pharm. Res. 16, 1722–1728.

Ohara, T., Kitamura, S., Kitagawa, T., Terada, K., 2005. Dissolution mechanism of poorly water-soluble drug from extended release solid dispersion system with ethylcellulose and hydroxypropylmethylcellulose. Int. J. Pharm. 302, 95–102.

Otsuka, M., Kato, F., Matsuda, Y., 2000. Comparative evaluation of the degree of indomethacin crystallinity by chemoinfometrical Fourier-transformed near-infrared spectroscopy and conventional powder X-ray diffractometry. AAPS Pharmsci. 2 (article 9).

Otsuka, M., Kato, F., Matsuda, Y., Ozaki, Y., 2003. Comparative determination of polymorphs of indomethacin in powders and tablets by chemometrical near-infrared spectroscopy and X-ray powder diffractometry. AAPS PharmSciTech 4 (article 19).

Roisnel, T., Rodriguez-Carvajal, J., 2001. WinPLOTR: a windows tool for powder diffraction pattern analysis. Mater. Sci. Forum 378–381, 118–123.

Serajuddin, A.T.M., 1999. Solid dispersions of poor water-soluble drugs: early promises, subsequent problems, and recent breakthroughs. J. Pharm. Sci. 88, 1058–1066.

Slavin, P., Sheen, D., Shepherd, E., 2002. Morphological evaluation of the β-polymorph of indomethacin. J. Crystal Growth 237–239, 300–305.

Sungthongjeen, S., Sriamornsak, P., Pitaksuteepong, T., Somsiri, A., 2004. Effect of degree of esterification of pectin and calcium amount on drug release from pectin-based matrix tablets. AAPS PharmSciTech 5 (article 9).

Takeuchi, H., Nagira, S., Yamamoto, H., Kawashima, Y., 2005. Solid dispersion particles of amorphous indomethacin with fine porous silica particles by using spray-drying method. Int. J. Pharm. 293, 155–164.

Taylor, L.S., Zografi, G., 1997. Spectroscopic characterization of interactions between PVP and indomethacin in amorphous molecular dispersions. Pharm. Res. 14, 1691–1698.

Van den Mooter, G., Wuyts, M., Blaton, N., Busson, R., Grobet, P., Augustijns, P., Kinget, R., 2001. Physical stabilization of amorphous ketoconazole in solid dispersions with polyvinylpyrrolidone K25. Eur. J. Pharm. Sci. 12, 261–269.

Yoshioka, M., Hancock, B., Zografi, G., 1994. Crystallization of indomethacin from the amorphous state below and above its glass transition temperature. J. Pharm. Sci. 83, 1700–1705.